Two novel bursting patterns in the Duffing system with multiple-frequency slow parametric excitations

Xiujing Han, Yi Zhang, Qinsheng Bi, and Jürgen Kurths

Citation: Chaos **28**, 043111 (2018); doi: 10.1063/1.5012519
View online: https://doi.org/10.1063/1.5012519
View Table of Contents: http://aip.scitation.org/toc/cha/28/4
Published by the American Institute of Physics

Two novel bursting patterns in the Duffing system with multiple-frequency slow parametric excitations

Xiujing Han,[1,2,3,a)] Yi Zhang,[1] Qinsheng Bi,[1] and Jürgen Kurths[2,3]
[1]*Faculty of Civil Engineering and Mechanics, Jiangsu University, Zhenjiang 212013, People's Republic of China*
[2]*Department of Physics, Humboldt University, Berlin 12489, Germany*
[3]*Potsdam Institute for Climate Impact Research, Potsdam 14473, Germany*

(Received 6 November 2017; accepted 26 March 2018; published online 11 April 2018)

This paper aims to report two novel bursting patterns, the turnover-of-pitchfork-hysteresis-induced bursting and the compound pitchfork-hysteresis bursting, demonstrated for the Duffing system with multiple-frequency parametric excitations. Typically, a hysteresis behavior between the origin and non-zero equilibria of the fast subsystem can be observed due to delayed pitchfork bifurcation. Based on numerical analysis, we show that the stable equilibrium branches, related to the non-zero equilibria resulted from the pitchfork bifurcation, may become the ones with twists and turns. Then, the novel bursting pattern turnover-of-pitchfork-hysteresis-induced bursting is revealed accordingly. In particular, we show that additional pitchfork bifurcation points may appear in the fast subsystem under certain parameter conditions. This creates multiple delay-induced hysteresis behavior and helps us to reveal the other novel bursting pattern, the compound pitchfork-hysteresis bursting. Besides, effects of parameters on the bursting patterns are studied to explore the relation of these two novel bursting patterns. *Published by AIP Publishing.*
https://doi.org/10.1063/1.5012519

Bursting oscillations are complex dynamical behaviors, characterized by large amplitude oscillations (LAOs) that alternate with small amplitude oscillations. Such oscillations are ubiquitous in multi-time-scale systems, i.e., dynamical systems whose variables evolve over several different time scales, frequently encountered in physics, chemistry, physiology, and other fields. Pitchfork-bifurcation-delay-induced hysteresis is one of the common routes to bursting. The resulting bursting pattern, however, often shows a simple dynamical behavior. The present paper focuses on interesting and relatively complicated bursting dynamics related to pitchfork-bifurcation-delay-induced hysteresis. As a result, two novel bursting patterns are revealed. We show that, under the action of multiple-frequency slow parametric excitations, pitchfork-bifurcation-delay-induced hysteresis may exhibit evolution modes with complex dynamical characteristics and, in particular, two interesting evolution modes of the hysteresis are explored. Based on this, we reveal by numerical analysis dynamical mechanisms of the two novel bursting patterns, analyze their respective dynamical characteristics, and explore relations between them.

I. INTRODUCTION

We consider the Duffing equation with multiple-frequency slow parametric excitations, given by

$$\ddot{x} + \delta\dot{x} - [\beta_1 \cos(\omega_1 t) + \beta_2 \cos(\omega_2 t)]x + x^3 = 0, \quad (1)$$

where $\delta\,(\delta > 0)$ is the damping and $\beta_1 \cos(\omega_1 t)$ and $\beta_2 \cos(\omega_2 t)$ are the slow parametric excitations. Here, we assume that the modulation frequencies $\omega_{1,2}$ ($\omega_{1,2} \ll 1$) are small enough so that there is a gap between the natural frequency of the system and the frequencies of excitations. Then, from the viewpoint of fast-slow dynamics, system (1) becomes the one with fast-slow characteristics.

When a system exhibits fast-slow characteristics, bursting may be created. Bursting is a typical representative of complex, fast-slow dynamical behavior and is frequently observed in various fields, such as biochemical reaction systems,[1,2] population dynamics,[3] nonlinear circuits,[4] and, in particular, in neuroscience where it plays an important role in information processing.[5–7] From a mathematical point of view, lots of bursting patterns are typically associated with the coexistence of different attractors.[8] Besides, bursting is also linked to canard phenomena,[9] singular Hopf bifurcations,[10] chaos crises,[11] speed escape of attractors,[12] and other dynamical mechanisms.[1,7,13,14]

Recently, bursting dynamics in systems with slow excitations has received much attention, leading to important results, such as the excitation amplitude and excitation frequency have been identified as two important factors affecting the properties of bursting.[15] In particular, the slow excitation (either parametric[16] or external[17]) can be interpreted as a slow variable, and based on this, a transformed phase diagram is obtained and applied to revealing dynamical mechanisms of bursting.[18] Besides, it is an interesting topic when more than one slow excitation is involved. For this case, the slow excitations may form a closed path in the plane/space of unfolding parameters, and in particular, bursting may be generated when the path passes through different

a)Electronic mail: xjhan@mail.ujs.edu.cn

areas where different attractors exist. Based on this, different bursting patterns and their classification have been investigated systematically and thoroughly, especially to mention Golubitsky *et al.*,[19] Osinga *et al.*,[20] and Saggio *et al.*[21] It has also been shown that systems with two slow excitations can be transformed into one with a single slow variable under certain conditions, and bursting can then be understood by studying the transformed fast-slow system.[22] Based on this, an interesting route to bursting, namely, the turnover of an S-shaped hysteresis curve related to fold bifurcations, has been recently revealed.[23]

In the absence of $\beta_2 \cos(\omega_2 t)$, system (1) becomes one with a single slow excitation. It has been shown that pitchfork bifurcation delay may exhibit due to a slow passage through a supercritical pitchfork bifurcation point.[24,25] In this case, the trajectory continues to follow the origin for some time, although it has become unstable. Then, a catastrophic transition from the unstable origin to the stable non-zero equilibria takes place when the delay terminates (e.g., see Fig. 1). In fact, such delay behavior leads to a hysteresis between the unstable origin and the stable none-zero equilibria and has been identified as playing a decisive role in the generation of pitchfork-hysteresis bursting.[26] Pitchfork-hysteresis bursting is a bursting pattern of point-point type, which often shows simple dynamical behaviors. In this paper, we focus on the influence of the additional excitation $\beta_2 \cos(\omega_2 t)$ on the pitchfork-hysteresis bursting. We show that, under the effects of $\beta_2 \cos(\omega_2 t)$, pitchfork-bifurcation-delay-induced hysteresis behaviors in system (1) may exhibit interesting dynamical characteristics which are quite different from those of the same system with a single slow excitation. Interesting and relatively complex bursting dynamics in system (1) is investigated, and as a result, two novel routes to bursting are revealed.

The rest of this paper is organized as follows: In Sec. II, two novel bursting patterns, i.e., the turnover-of-pitchfork-hysteresis-induced bursting and the compound pitchfork-hysteresis bursting, are presented. Next, we investigate via intensive numerical analysis dynamical mechanisms of both bursting patterns in Secs. III and IV, respectively, where some important characteristics of the bursting patterns are also analyzed. Then, in Sec. V, we consider effects of parameters on the bursting and explore the transitions between the two novel bursting patterns. Finally, in Sec. VI, we conclude the paper.

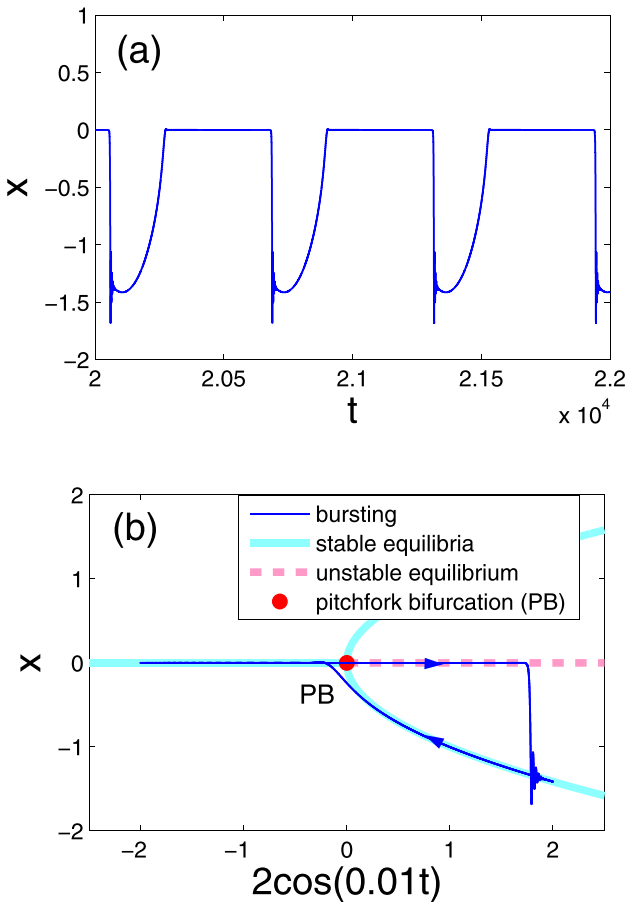

FIG. 1. Pitchfork-hysteresis bursting of point-point type induced by a delayed pitchfork bifurcation in the system $\ddot{x} + \delta\dot{x} - [\beta_1 \cos(\omega_1 t)]x + x^3 = 0$, where $\delta = 0.5$, $\beta_1 = 2$, and $\omega_1 = 0.01$ (a), and fast-slow analysis of the pitchfork-hysteresis bursting (b). Here the slow variable is $\beta_1 \cos(\omega_1 t)$. The bifurcation diagram is obtained based on the fast subsystem $\ddot{x} + \delta\dot{x} - \gamma x + x^3 = 0$, where γ is the control parameter. At the critical value $\gamma_{PB} = 0$, a supercritical pitchfork bifurcation *PB* takes place.

II. TWO NOVEL BURSTING PATTERNS

In this section, we explore novel bursting dynamics of the Duffing system (1). Here, we focus on the influence of $\beta_2 \cos(\omega_2 t)$ on the bursting in Fig. 1. The two resultant bursting patterns, as typical representations of novel bursting dynamics of the system, will be shown.

We start by analyzing bursting in system (1) for the case when $\omega_2 = \omega_1 = O(\varepsilon)$ where $\varepsilon \ll 1$. Obviously, system (1) then becomes one with a single slow excitation whose amplitude is $\beta_1 + \beta_2$; thus, bursting represented by the one shown in Fig. 1(a) is obtained. We see that the bursting shows a fast-slow characteristic, characterized by slow asymptotic behaviors and pitchfork-bifurcation-delay-induced catastrophic transitions from the unstable origin to the non-zero equilibrium point attractors [e.g., see Fig. 1(b)].

When $\omega_2 \neq \omega_1$, however, the case becomes quite different. Interesting dynamical characteristics may appear in the bursting for this case, and even novel bursting patterns are created. Figure 2 shows a group of bursting patterns in

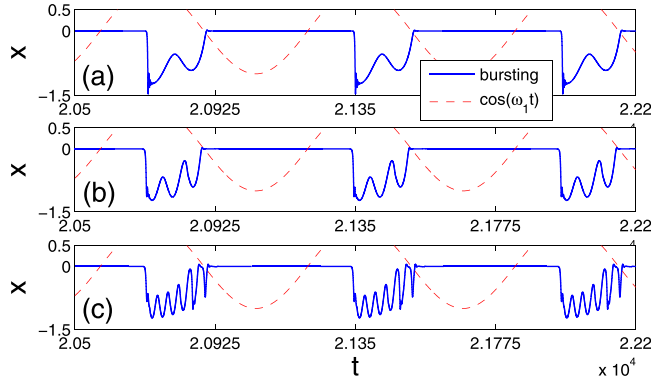

FIG. 2. Turnover-of-pitchfork-hysteresis-induced bursting patterns in system (1) for (a) $\omega_2 = 0.05$, (b) $\omega_2 = 0.1$, and (c) $\omega_2 = 0.2$. Other parameters are fixed at $\delta = 0.5$, $\beta_1 = 1$, $\omega_1 = 0.01$, and $\beta_2 = 0.5$. The function $\cos(\omega_1 t)$ is superimposed to clearly show that $\omega_B = \omega_1$.

system (1) with increasing values of ω_2 for $\delta = 0.5$, $\beta_1 = 1$, $\omega_1 = 0.01$, and $\beta_2 = 0.5$. It is seen that the bursting exhibits large-amplitude oscillations (LAOs), the active phase of bursting, which alternate with small-amplitude oscillations, the rest phase of bursting. In fact, such transitions between active and rest phases are also observed in the bursting pattern shown in Fig. 1(a). However, the bursting patterns in Fig. 2 exhibit some characteristics which are quite different from those of in Fig. 1(a), i.e., more LAOs than one are generated in each period of the bursting. In particular, increasing numbers of LAOs are observed in the active phase of bursting as the frequency ω_2 increases. Two important problems then arise naturally: One is what is the dynamical mechanism underlying the appearance of increasing numbers of LAOs, and the other is how to calculate the frequency of LAOs. These two problems are interrelated, and they will be investigated in Sec. III.

Besides the bursting in Fig. 2, another group of interesting bursting is observed in system (1). Some examples of the bursting with increasing values of ω_2 are shown in Fig. 3, where $\beta_2 = 3$ and other parameters are the same as those in Fig. 2. An increasing number of active and rest phases are generated in each period of the bursting; however, the number of LAOs in each active phase remains unchanged. These characteristics are novel and quite different compared to those of the bursting patterns in Figs. 1 and 2. Dynamical mechanisms of these bursting patterns will be investigated in Sec. IV, where some important dynamical characteristics of the bursting will also be explored.

III. TURNOVER-OF-PITCHFORK-HYSTERESIS-INDUCED BURSTING

In this section, we explore the first novel bursting pattern, i.e., the bursting shown in Fig. 2, called "turnover-of-pitchfork-hysteresis-induced bursting." It will be found to be linked to the fact that the stable non-zero equilibrium branches bifurcated from the pitchfork bifurcation point may become winding and tortuous.

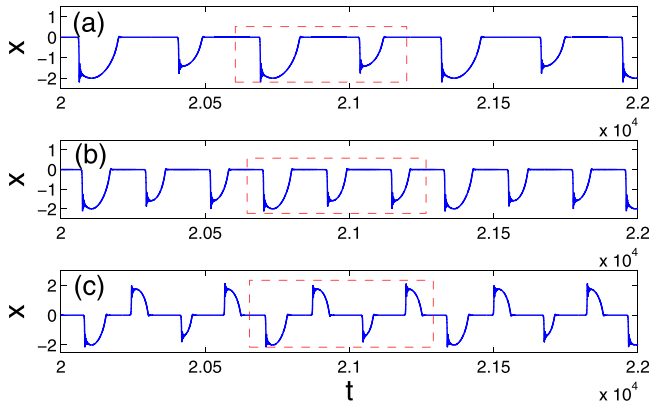

FIG. 3. Compound pitchfork-hysteresis bursting patterns in system (1) for (a) $\omega_2 = 0.02$, (b) $\omega_2 = 0.03$, and (c) $\omega_2 = 0.04$. The parameters δ, β_1 and ω_1 are the same as those in Fig. 2, and β_2 is fixed at $\beta_2 = 3$. The red rectangles indicate one period of the bursting.

A. Dynamical mechanism of bursting

As we have noted, the parametric excitations vary slowly, and there is a gap between the natural frequency of the Duffing system and the frequencies of excitations. Therefore, system (1) is in fact a fast-slow system with two slow variables (i.e., the slow excitations), which can be transformed into one with a single slow variable according to the method recently developed in Ref. 22. Then, bursting observed in system (1) can be understood by the classical fast subsystem analysis of the transformed fast-slow system. Moreover, the transformed fast-slow system can be obtained according to the relation between the frequencies of the parametric excitations.

Note that the frequency ω_2 is an integer multiple of the frequency ω_1 (Fig. 2). Therefore, we obtain the transformed fast-slow system

$$\ddot{x} + \delta\dot{x} - \left[\beta_1 g(t) + \beta_2 f_n^*(g(t))\right]x + x^3 = 0, \tag{2}$$

where $g(t) = \cos(\omega_1 t)$ is the only slow variable of the system, and $f_n^*(x)$ resulted from $\cos(\omega_2 t) = f_n^*(\cos(\omega_1 t))$ is the polynomial function

$$f_n^*(x) = C_n^0 x^n - C_n^2 x^{n-2}(1-x^2) + C_n^4 x^{n-4}(1-x^2)^2 - \cdots + i^m C_n^m x^{n-m}(1-x^2)^{\frac{m}{2}}, \tag{3}$$

in which $m\,(m \le n)$ is the maximum even number not larger than n. Freezing the slow variable $g(t)$ in system (2) leads to the fast subsystem, given by

$$\ddot{x} + \delta\dot{x} - \left[\beta_1\gamma + \beta_2 f_n^*(\gamma)\right]x + x^3 = 0, \tag{4}$$

where γ is the control parameter.

We now investigate dynamical mechanisms leading to the bursting patterns. We consider the bursting shown in Fig. 2(a). Note that $\omega_2 = 5\omega_1 = 0.05$, so we have the slow variable $g(t) = \cos(0.01t)$ and the fast subsystem $\ddot{x} + \delta\dot{x} - [\beta_1\gamma + \beta_2 f_5^*(\gamma)]x + x^3 = 0$, where γ is the control parameter. Here, δ and $\beta_{1,2}$ are the same as those in Fig. 2. This fast subsystem exhibits a pitchfork bifurcation, giving rise to two stable branches of non-zero equilibria. Interestingly, both of the non-zero branches now become the ones with twists and turns, characterized by two extreme points appearing on each of the non-zero branches [see Fig. 4(a)]. Compared to the bursting pattern in Fig. 1(a), additional LAOs in the active phase are thus created [see Figs. 2(a) and 4(b)].

Furthermore, we find that an increasing number of extreme points are created on the stable branches of non-zero equilibria if we increase the frequency ω_2 (ω_1 remains unchanged). For example, when $\omega_2 = 0.1$, four extreme points are observed on each of the non-zero branches [Fig. 4(c)]; when $\omega_2 = 0.2$, six extreme points are observed on each of the non-zero branches [Fig. 4(e)]. This explains why there are an increasing number of LAOs observed in the active phase of bursting as the frequency ω_2 increases [Figs. 2, 4(b), 4(d), and 4(f)].

In our recent paper,[23] we showed that the stable upper and lower branches of equilibrium points, related to an S-shaped equilibrium hysteresis curve with two fold bifurcation

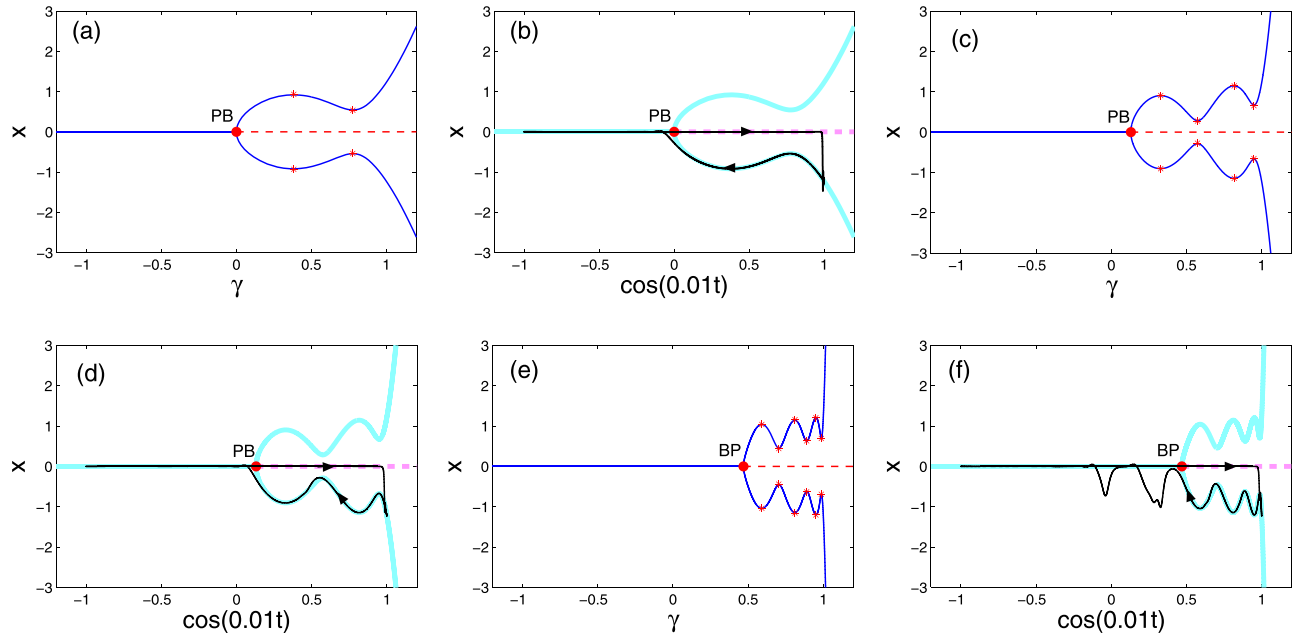

FIG. 4. Fast-slow analysis of the bursting patterns in Fig. 2. The numerical simulations shown in (a) and (b), (c) and (d), and (e) and (f) are related to the bursting in Figs. 2(a), 2(b), and 2(c), respectively. The related fast subsystems are $\ddot{x} + \delta\dot{x} - [\beta_1\gamma + \beta_2 f_n^*(\gamma)]x + x^3 = 0$, where $n = 5, 10$, and 20, respectively, γ is the control parameter, and the other parameters are the same as those in Fig. 2. The slow variable is $g(t) = \cos(0.01t)$. The red stars indicate extreme points of the non-zero branches.

points, may rise and fall, which gives rise to extreme points appearing on the stable branches of the equilibrium points, and a bursting pattern, i.e., the so-called turnover-of-hysteresis-induced bursting related to fold bifurcations, is created. As we have seen, the turnover-of-hysteresis phenomena of stable equilibrium branches reported here, however, are related to a different bifurcation type, i.e., the pitchfork bifurcation. Considering the bifurcation type involved, we refer to the bursting patterns in Fig. 2 as "turnover-of-pitchfork-hysteresis-induced bursting."

We close this subsection by pointing out that, with further increase in the frequency ω_2, unusual impulsive phenomena are observed at the end of the active phase of bursting [Figs. 5(a) and 5(b)]. Our numerical results further show that, near the pitchfork bifurcation point, the non-zero equilibrium branches may become steep [Fig. 5(c)], i.e., the supercritical pitchfork bifurcation, a kind of soft bifurcation, now exhibits some characteristics similar to those of hard bifurcations. Therefore, a sharp transition from the non-zero equilibria to the origin is created. It is clear that the impulsive phenomena observed in bursting patterns seem to be related to such a sharp transition [Fig. 5(c)]. However, how large the frequency ω_2 is allowed to be to observe bursting showing impulsive phenomena is hazy and needs further investigation.

B. Frequency of LAOs

In what follows, we analyze frequency properties of the turnover-of-pitchfork-hysteresis-induced bursting. As we have seen in Fig. 2, two frequency components are observed in each bursting pattern. One is the frequency of the LAOs (denoted by ω_L), and the other is the frequency of the bursting (denoted by ω_B). The fast-slow analysis in Fig. 4 clearly shows that bursting has the same frequency as that of the slow variable $g(t) = \cos(\omega_1 t)$, i.e., $\omega_B = \omega_1$ (see Fig. 2). So, here we focus on the frequency ω_L.

As we analyzed in Ref. 27, here we adopt the idea of using bifurcation analysis of the fast subsystem to explore ω_L by considering the two parametric excitations as a whole.[19] From this point of view, it means that system (1) can then be considered as a fast-slow system with a single slow variable. However, the slow variable $g(t)$ for this case is a complex one, i.e., $g(t) = \beta_1 \cos(\omega_1 t) + \beta_2 \cos(\omega_2 t)$, which exhibits a complex control mode for the fast subsystem

$$\ddot{x} + \delta\dot{x} - \gamma x + x^3 = 0, \tag{5}$$

where $\gamma = g(t)$ is the control parameter. When $g(t)$ increases through the pitchfork bifurcation point $\gamma_{PB} = 0$, a similar pitchfork bifurcation delay behavior may be created. The termination of bifurcation delay leads to a sharp transition to one of the stable non-zero equilibria (say, the upper equilibrium E_u) [see Fig. 6(a)]. Then an evolution, related to the bursting trajectory which traces E_u, takes place. As shown in Fig. 6(a), this evolution can be divided into two parts: one is the part from A to B and the other is from B to PB.

Here, we take the part from B to PB as an example to show that $\omega_L = \omega_2$. Note that $\omega_2 = n\omega_1$ and β_2 is relatively small compared to β_1. Therefore, the presence of $\beta_2 \cos(\omega_2 t)$ leads the slow variable $g(t)$ to fluctuate narrowly around $\beta_1 \cos(\omega_1 t)$ (see Fig. 7). That is, during the evolution part from B to PB, $g(t)$ alternates between decreases and increases. Then, the traced attractor E_u shows values alternating between decreases and increases accordingly. As a result, the bursting trajectory exhibits amplitude-modulated oscillations during the evolution part from B to PB [see Fig. 6(b)]. Based on the above analysis, we see that the amplitude-modulated

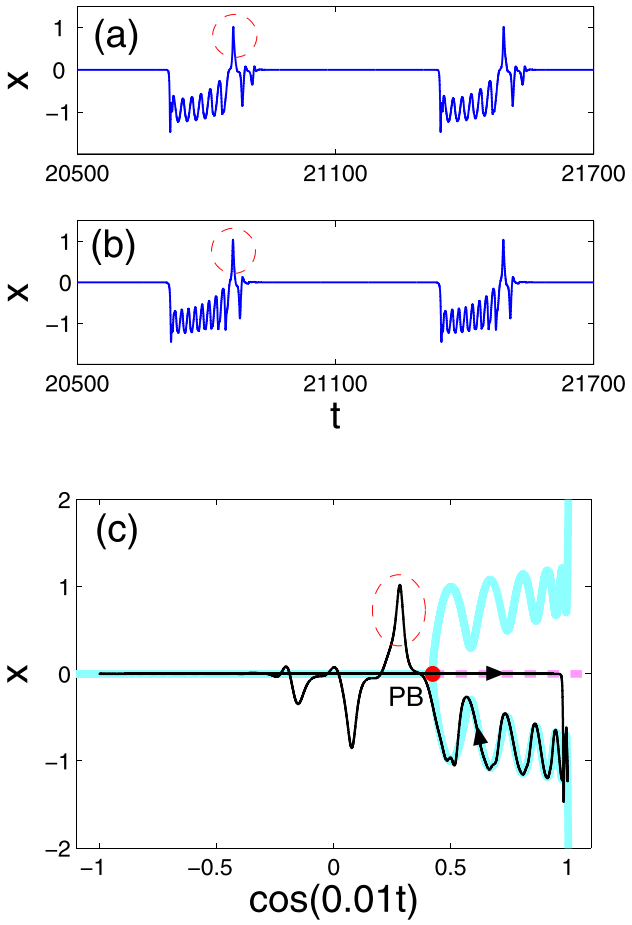

FIG. 5. Turnover-of-pitchfork-hysteresis-induced bursting patterns (a) and (b) and fast-slow analysis of the bursting (c). (a) $\omega_2 = 0.3$; (b) $\omega_2 = 0.4$. The other parameters in (a) and (b) are the same as those in Fig. 2. (c) Fast-slow analysis of the bursting in (a). Here, the slow variable is $g(t) = \cos(0.01t)$, and the fast subsystem is $\ddot{x} + \delta\dot{x} - [\beta_1\gamma + \beta_2 f^*_{30}(\gamma)]x + x^3 = 0$, where γ is the control parameter and other parameters are the same as those in (a). The red circles give a clear view of the impulsive phenomena.

oscillations (i.e., the LAOs) have the same frequency as those of the transitions between decreases and increases that $g(t)$ exhibits. On the other hand, note that such transitions are decided by the additional excitation $\beta_2\cos(\omega_2 t)$, and therefore, one may conclude that LAOs and $\beta_2\cos(\omega_2 t)$ have the same oscillation frequency, i.e., $\omega_L = \omega_2$ (e.g., see Fig. 8).

IV. COMPOUND PITCHFORK-HYSTERESIS BURSTING

In this section, we consider the second novel bursting pattern in Fig. 3. We first explore the dynamical mechanisms of the bursting. We will show that this bursting pattern, which we call compound pitchfork-hysteresis bursting, is a kind of complex bursting, because it is made up of several pitchfork-hysteresis bursting sequentially. Afterwards, the number of simple bursting patterns, related to the number of LAOs, in each period of the compound bursting will be explored.

A. Dynamical mechanism of bursting

We analyze the bursting shown in Fig. 3(a). Note that $\omega_1 = 0.01$ and $\omega_2 = 0.02$, so, by using the method analyzed

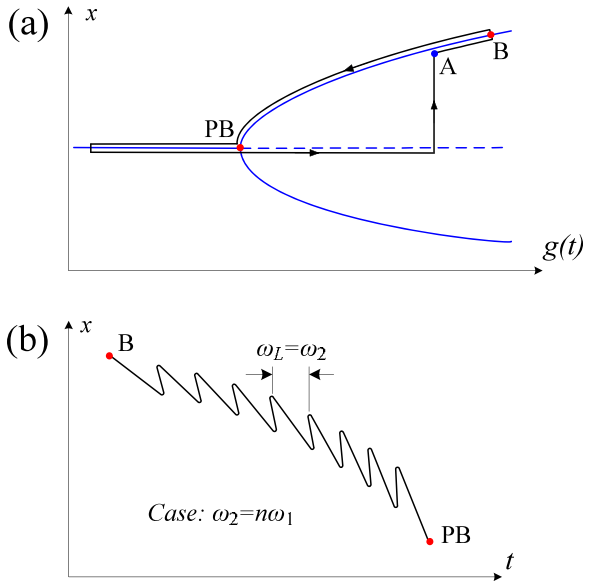

FIG. 6. (Schematic diagrams) Evolution of the bursting for $\omega_2 = n\omega_1$ where n is a positive integer (a) and its fragment which is from B to PB (b). Here, A is the point where the evolution related to tracing the stable upper branch starts, B is the maximum of the slow variable $g(t) = \beta_1\cos(\omega_1 t) + \beta_2\cos(\omega_2 t)$, and PB is a pitchfork bifurcation point of the fast subsystem (5).

in Subsection III A, we get the slow variable $g(t) = \cos(0.01t)$ and the fast subsystem $\ddot{x} + \delta\dot{x} - [\beta_1\gamma + \beta_2 f^*_2(\gamma)]x + x^3 = 0$, where $\gamma = g(t) = \cos(0.01t)$ is the control parameter. As shown in Fig. 9(a), the bifurcation diagram of this fast subsystem exhibits two pitchfork bifurcation points within the parameter interval $\gamma \in [-1, 1]$. Then, we overlay the bifurcation diagram with the transformed phase diagram of the bursting. We see that, when the slow variable is "switched on," the two pitchfork bifurcation points lead to two pitchfork-hysteresis bursting patterns, which are connected by the rest phase of each pitchfork-hysteresis bursting [Fig. 9(b)]. Therefore, a complex bursting pattern, consisting of two simple bursting patterns of pitchfork-hysteresis type in each period, is created [see Fig. 3(a)].

Next, we consider the bursting in Fig. 3(b). Because of $\omega_1 = 0.01$ and $\omega_2 = 0.03$, we have the fast subsystem

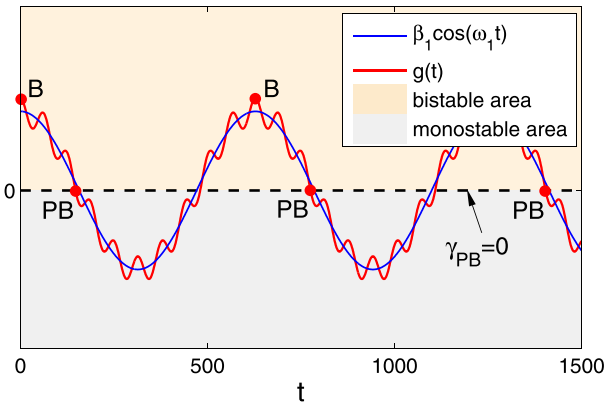

FIG. 7. (Schematic diagram) The slow variable $g(t)$ fluctuates narrowly around $\beta_1\cos(\omega_1 t)$ because the additional excitation $\beta_2\cos(\omega_2 t)$ has a relatively small amplitude and a relatively high frequency. Dashed line: pitchfork bifurcation ($\gamma_{PB} = 0$), bistable area: non-zero equilibrium point attractors, monostable area: stable origin.

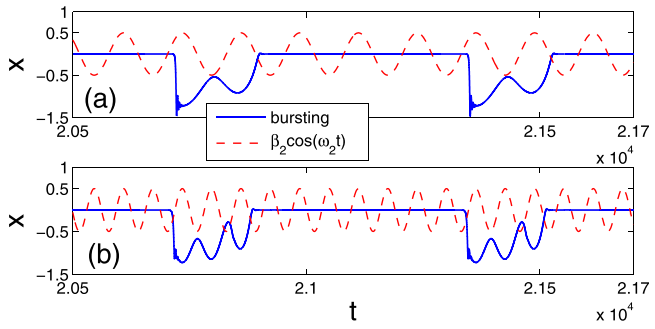

FIG. 8. Superposition of the turnover-of-pitchfork-hysteresis-induced bursting and the excitation $\beta_2\cos(\omega_2 t)$ gives a clear view that $\omega_L = \omega_2$. The parameters in (a) and (b) are the same as those in Figs. 2(a) and 2(b), respectively.

$\ddot{x} + \delta\dot{x} - [\beta_1\gamma + \beta_2 f_3^*(\gamma)]x + x^3 = 0$. Then, an additional pitchfork bifurcation point is created, and in all, three pitchfork bifurcation points are observed within $\gamma \in [-1, 1]$ [Fig. 9(c)]. This thus leads to a complex bursting pattern, containing three simple bursting patterns of pitchfork-hysteresis type [Figs. 9(d) and 3(b)].

For the bursting in Fig. 3(c), it is easy to check that the associated fast subsystem is $\ddot{x} + \delta\dot{x} - [\beta_1\gamma + \beta_2 f_4^*(\gamma)]x + x^3 = 0$, where $\gamma = \cos(0.01t)$ is the control parameter. For this case, as shown in Fig. 9(e), four pitchfork bifurcation points can be observed within $\gamma \in [-1, 1]$, and therein lies the generation of four simple bursting patterns of pitchfork-hysteresis type in each period of the complex bursting [see Figs. 9(f) and 3(c)].

Delayed pitchfork bifurcation is one of the most common bifurcations in relation to bursting. It may lead to a fast transition from an unstable equilibrium to various attractors, which can be equilibria, periodic orbits, or chaos. Accordingly, different types of bursting can therefore be created, e.g., bursting of point-point type,[19,28] bursting of point-cycle type,[29,30] and bursting of point-chaos type.[31,32] The bursting patterns shown in Fig. 3 are, of course, of point-point type, because they result from transitions among equilibria of the system. However, the bursting patterns reported here show some compound dynamical characteristics, which are quite different from those reported in previous works, i.e., each of the bursting is composed of several simple bursting patterns of pitchfork-hysteresis type. Considering the compound dynamical characteristics, the bursting patterns in Fig. 3 are called "compound pitchfork-hysteresis bursting."

B. Numbers of LAOs

We have demonstrated that simple pitchfork-hysteresis bursting patterns are observed in each period of the compound pitchfork-hysteresis bursting. In this subsection, the method used in Subsection III B is applied to analyzing the number of pitchfork-hysteresis bursting patterns in the compound bursting, and this in fact is related to the number of LAOs observed in each period of the compound bursting.

By considering the slow excitations as a whole, we obtain the slow variable $g(t) = \beta_1\cos(\omega_1 t) + \beta_2\cos(\omega_2 t)$ and the fast subsystem (5). Note that the relation $\omega_2 = n\omega_1$ remains unchanged. So, one cycle of $\beta_1\cos(\omega_1 t)$ means n cycles of $\beta_2\cos(\omega_2 t)$, which further indicates that $\beta_2\cos(\omega_2 t)$ will increase through γ_{PB} n times during each period of $\beta_1\cos(\omega_1 t)$. Besides, as shown in Fig. 3, compared to the amplitude β_1, the amplitude β_2 is so large that the slow variable $g(t)$ may inherit the properties from $\beta_2\cos(\omega_2 t)$, i.e., the slow variable $g(t)$ also increases through γ_{PB} n times during one period of $\beta_1\cos(\omega_1 t)$ (Fig. 10). In particular, an increase through γ_{PB} that $g(t)$ exhibits may lead to a pitchfork-hysteresis bursting pattern, and therefore, n pitchfork-hysteresis bursting patterns are observed in the compound bursting. Besides, note that each pitchfork-hysteresis bursting means one oscillation with a large amplitude. So, n LAOs are observed in each period of the compound bursting for the case when ω_2 is an integer multiple of ω_1.

Some examples of the compound bursting related to the above analysis can be found in Fig. 3. For example, when

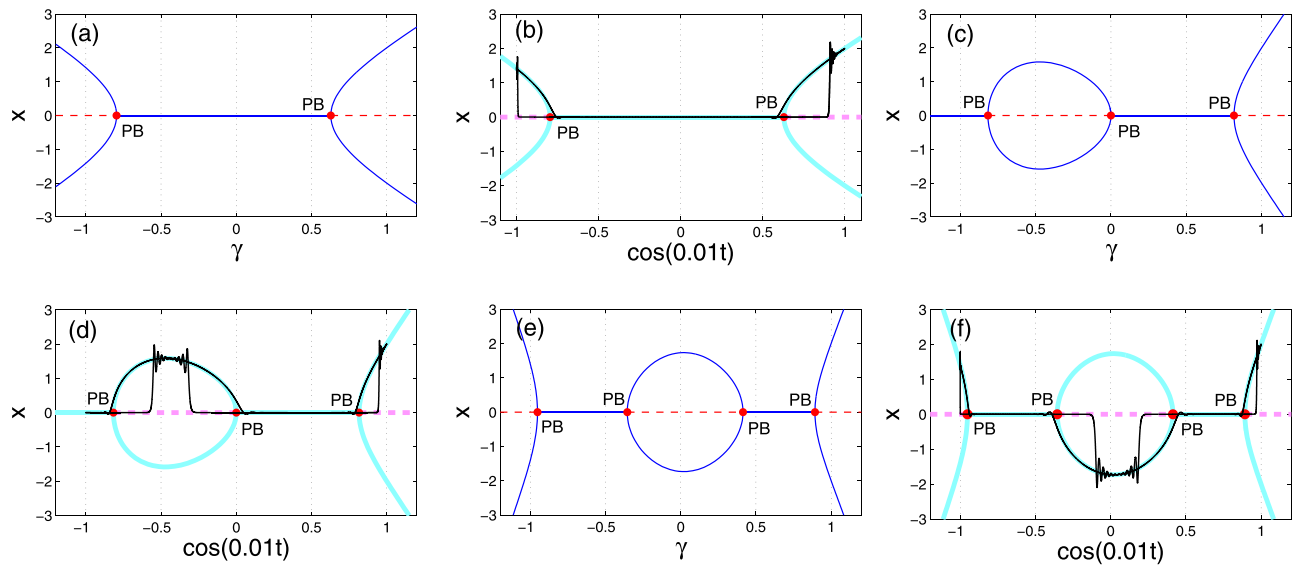

FIG. 9. Fast-slow analysis of the bursting patterns in Fig. 3. The simulations shown in (a) and (b), (c) and (d), and (e) and (f) are related to the bursting in Figs. 3(a), 3(b), and 3(c), respectively. The fast subsystems are $\ddot{x} + \delta\dot{x} - [\beta_1\gamma + \beta_2 f_n^*(\gamma)]x + x^3 = 0$, where $\delta = 0.5$, $\beta_1 = 1$, $\beta_2 = 3$, γ is the control parameter, and $n = 2$, 3, and 4, respectively; the slow variable is $g(t) = \cos(0.01t)$.

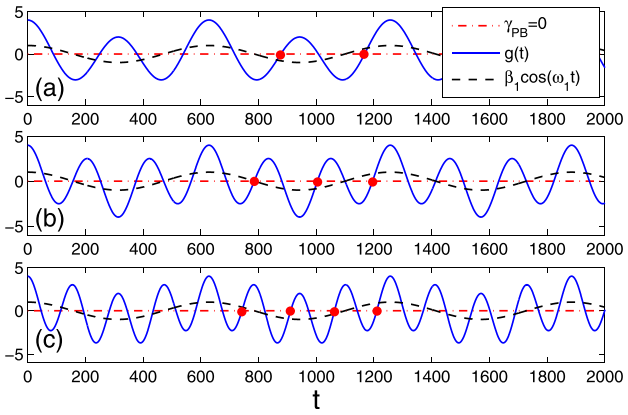

FIG. 10. Evolutions of $\beta_1\cos(\omega_1 t)$ and $g(t)=\beta_1\cos(\omega_1 t)+\beta_2\cos(\omega_2 t)$ when $\omega_2=n\omega_1$ for (a) $n=2$, (b) $n=3$, and (c) $n=4$. The parameters are fixed at $\beta_1=1$, $\beta_2=3$, and $\omega_1=0.01$. During one cycle of its evolution, $g(t)$ is able to increase through γ_{PB} two, three, and four times (marked by red points), respectively.

$\omega_2=2\omega_1$, two LAOs are observed in each period of the compound bursting [see Fig. 3(a)]; when $\omega_2=3\omega_1$ and $4\omega_1$, respectively, three and four LAOs are generated in each period of the compound bursting, respectively [see Figs. 3(b) and 3(c)]. With further increase in n, an increasing number of LAOs are expected. Figure 11 shows the cases when $\omega_2=5\omega_1$ and $10\omega_1$, respectively. We indeed find there that five and ten LAOs are observed in each period of the compound bursting, respectively, which further confirms the validity of the above analysis.

V. RELATION BETWEEN THE NOVEL BURSTING PATTERNS

We have demonstrated that varying the excitation frequencies may lead to quantitative changes of the novel bursting patterns. In this section, we focus on the effects of parameters on the bursting, and explore the relation between both novel bursting patterns.

To begin with, we consider effects of the parameter δ on the bursting. It is easy to check that the stabilities of the equilibrium branches of the fast subsystem $\ddot{x}+\delta\dot{x}-[\beta_1\gamma+\beta_2 f_n^*(\gamma)]x+x^3=0$, where γ is the control parameter, are independent of δ. Moreover, the stable equilibrium branches can be nodes or focuses, which rely on δ. Therefore, different values of δ may lead to similarly shaped bursting patterns

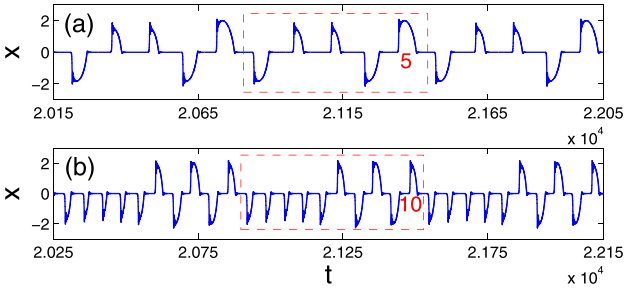

FIG. 11. Compound pitchfork-hysteresis bursting in system (1) for (a) $\omega_2=0.05$ and (b) $\omega_2=0.1$. Other parameters are the same as those in Fig. 3. The red numbers 5 and 10 indicate the number of LAOs in each period of the compound bursting.

with the same dynamical mechanism, i.e., the turnover-of-pitchfork-hysteresis-induced bursting. Similarly, we find that the result is also true for the compound pitchfork-hysteresis bursting. Therefore, varying δ will not lead to qualitative changes of the two novel bursting patterns.

However, it may be quite different if we vary the excitation amplitudes. As we have pointed out in Subsection IV B, the compound pitchfork-hysteresis bursting, consisting of n pitchfork-hysteresis bursting patterns, is created due to the fact that the slow variable $g(t)=\beta_1\cos(\omega_1 t)+\beta_2\cos(\omega_2 t)$ (here $\omega_2=n\omega_1$) is able to inherit the properties from $\beta_2\cos(\omega_2 t)$, and this relies on the values of the amplitudes $\beta_{1,2}$, i.e., such a regime may be destroyed if the amplitudes vary. Therefore, the excitation amplitudes have strong effects on the bursting behaviors.

Here, we take the compound bursting shown in Fig. 11(a) as a typical example to explore qualitative changes of the bursting as the amplitude β_2 varies. Figure 12 shows a fast-slow analysis of the compound pitchfork-hysteresis bursting in Fig. 11(a). It is seen that the generation of this compound bursting is related to the five pitchfork bifurcation points within the parameter interval $\gamma\in[-1,1]$. In order to detect qualitative changes in the bursting behavior, a two parameter bifurcation set of the fast subsystem $\ddot{x}+\delta\dot{x}-[\beta_1\gamma+\beta_2 f_5^*(\gamma)]x+x^3=0$ with respect to the slow variable

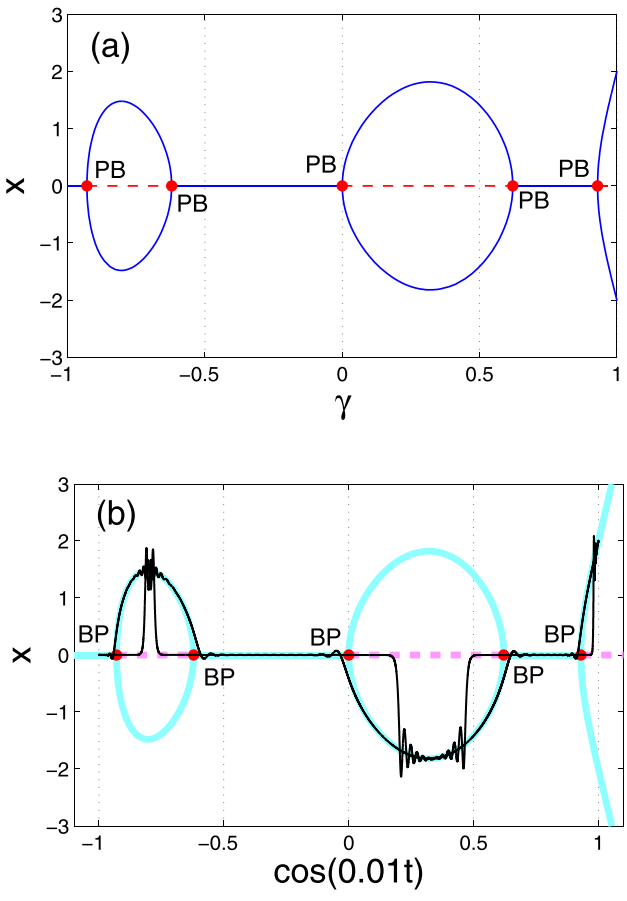

FIG. 12. Fast-slow analysis of the compound pitchfork-hysteresis bursting in Fig. 11(a). The bifurcation diagram is obtained based on the fast subsystem $\ddot{x}+\delta\dot{x}-[\beta_1\gamma+\beta_2 f_5^*(\gamma)]x+x^3=0$, where γ is the control parameter, and the other parameters are the same as those in Fig. 11(a). The slow variable is $g(t)=\cos(0.01t)$.

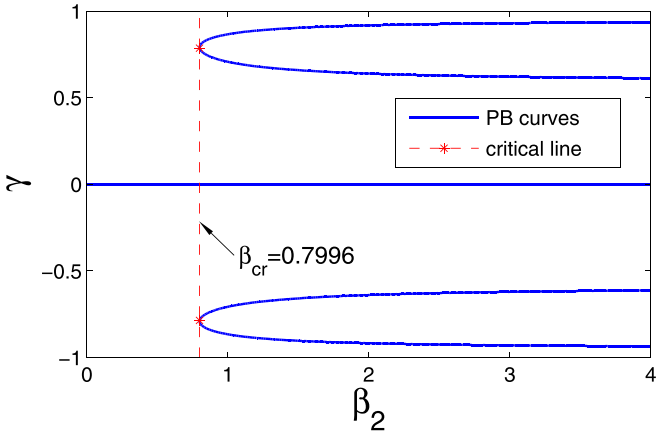

FIG. 13. Bifurcation set of the fast subsystem $\ddot{x} + \delta\dot{x} - [\beta_1\gamma + \beta_2 f_5^*(\gamma)]x + x^3 = 0$ with respect to γ and β_2. The parameters δ and β_1 are the same as those in Fig. 12.

γ and the amplitude β_2 is shown in Fig. 13, where the critical line $\beta_{cr} = 0.7996$ is also added. At the right part of β_{cr}, there are five pitchfork bifurcation curves, which cause the generation of the compound pitchfork-hysteresis bursting represented in Fig. 11(a). At the left part, however, only one pitchfork bifurcation curve appears. Therefore, the compound pitchfork-hysteresis bursting will disappear when β_2 decreases though β_{cr}; instead, a turnover-of-pitchfork-hysteresis-induced bursting pattern, represented by the one shown in Fig. 2(a), is created. Based on the above analysis, we conclude that the two novel bursting patterns are closely related, and they can transform into each other by varying the excitation amplitudes.

We would like to point out that lots of numerical simulations show that the delay-induced pitchfork hysteresis behaviors that the compound bursting patterns rely on are heavily dependent on the values of the amplitudes. For example, when β_2 decreases to 1.58, one of the five pitchfork bifurcation points does not show a delay-induced hysteresis behavior [Fig. 14(a1)]; when β_2 decreases to 1.4, an additional pitchfork bifurcation point does not show a delay-induced hysteresis behavior [Fig. 14(b1)]; when β_2 decreases to 1.04, three pitchfork bifurcation points do not show a delay-induced hysteresis behavior [Fig. 14(c1)]. Note that each delay-induced hysteresis behavior means a simple pitchfork-hysteresis bursting pattern, which further indicates an oscillation with a large amplitude. Accordingly, a decreasing number of LAOs are observed in the compound pitchfork-hysteresis bursting [Figs. 11(a), 14(a2), 14(b2), and 14(c2)]. When the amplitude β_2 decreases through β_{cr}, the compound pitchfork-hysteresis bursting disappears, and the transition to the turnover-of-pitchfork-hysteresis-induced bursting takes place eventually (e.g., see Fig. 15). According to the above analysis, we can conclude that, generally, the compound pitchfork-hysteresis bursting and the turnover-of-pitchfork-hysteresis-induced bursting cannot be transformed into each other immediately, and the transition between them often shows a complex evolution course, during which, the number of LAOs in each period of the compound bursting varies with the amplitudes.

Besides, our numerical simulations demonstrate that each of the pitchfork bifurcation points generates a delay-induced hysteresis behavior as long as the excitation amplitude β_2 is large enough [see Figs. 9(b), 9(d), 9(f), and 12(b)]. However, how large the excitation amplitude is allowed to be to observe all the pitchfork bifurcation points showing delay-induced hysteresis behavior is a difficult problem, and needs to be further studied.

VI. CONCLUSION AND DISCUSSION

Pitchfork-hysteresis bursting is a common bursting pattern in the Duffing system with a single slow parametric excitation. In this paper, the influence of an additional slow parametric excitation on the pitchfork-hysteresis bursting has been explored numerically. As a result, two novel bursting patterns, the turnover-of-pitchfork-hysteresis-induced bursting and the compound pitchfork-hysteresis bursting, have been revealed in the Duffing system with multiple-frequency slow parametric excitations.

Typically, the pitchfork-hysteresis bursting is related to hysteresis phenomena resulting from a pitchfork bifurcation delay behavior. Our study shows that, under the effects of an additional slow parametric excitation, the original hysteresis behaviors exhibit interesting dynamical characteristics. Two evolution modes of hysteresis behaviors have been found to be related to the generation of the novel bursting patterns under the condition that the frequency of the additional excitation is an integer multiple of the frequency of the original excitation. One is related to the case when the non-zero

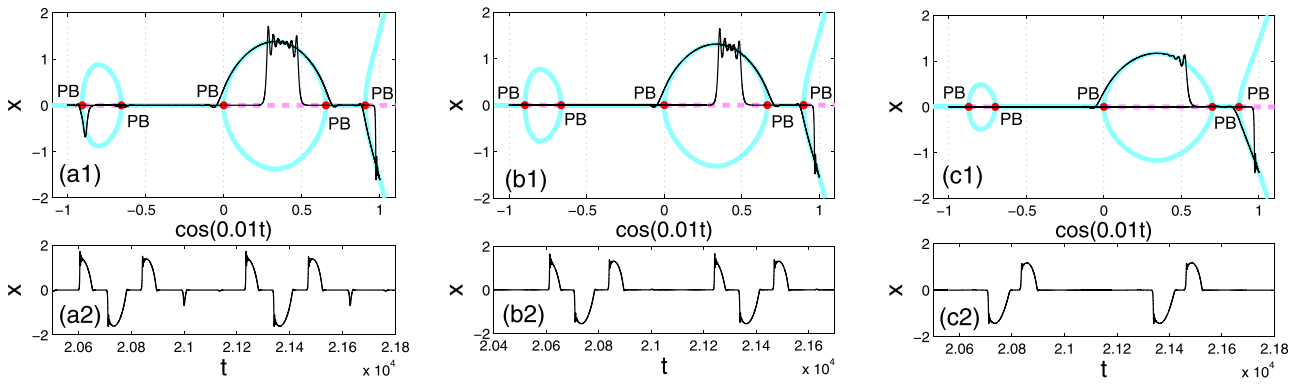

FIG. 14. The number of LAOs (denoted by n) observed in each period of the compound pitchfork-hysteresis bursting decreases with the amplitude β_2. (a1) and (a2) $\beta_2 = 1.58$, $n = 4$; (b1) and (b2) $\beta_2 = 1.4$, $n = 3$; (c1) and (c2) $\beta_2 = 1.04$, $n = 2$. The other parameters are the same as those in Fig. 10(a).

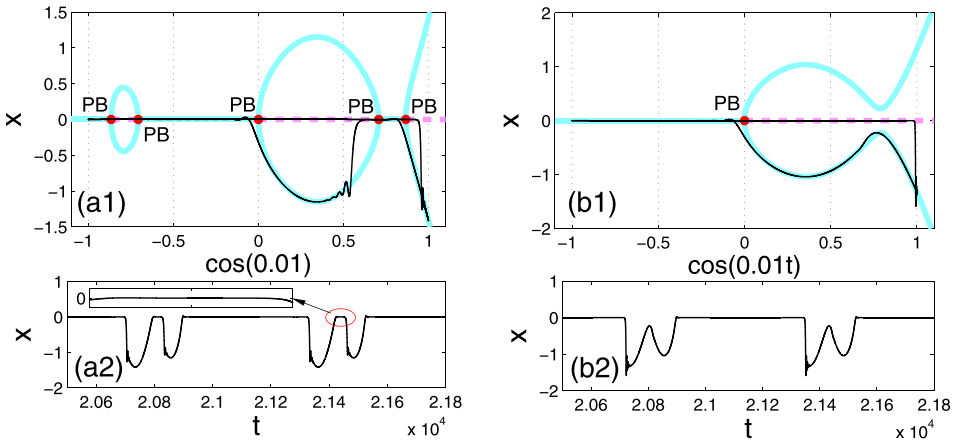

FIG. 15. Bursting patterns near the critical point β_{cr}. (a1) and (a2) Compound pitchfork-hysteresis bursting consisting of two pitchfork-hysteresis bursting patterns ($\beta_2 = 1$); (b1) and (b2) turnover-of-pitchfork-hysteresis-induced bursting ($\beta_2 = 0.75$). The other parameters are the same as those in Fig. 13. The inset in (a2) gives a clear view that the bursting pattern in (a2) is different from the one in (b2).

equilibrium hysteresis curves become the ones with twists and turns, characterized by extreme points appearing on the stable non-zero branches. This gives rise to the turnover-of-pitchfork-hysteresis-induced bursting whose active phase has the same frequency as that of the additional slow excitation. The other is related to the case when additional pitchfork bifurcation points appear on the equilibrium hysteresis curves, which account for the generation of the compound pitchfork-hysteresis bursting. The number of pitchfork-hysteresis bursting patterns in the compound pitchfork-hysteresis bursting is decided by the ratio of the additional excitation frequency to the original excitation frequency for the case when the amplitude of the additional excitation is large enough.

We have also investigated effects of the parameters on the bursting patterns. The excitation amplitudes have been identified as crucial factors affecting the properties of bursting patterns. There may be a mutual transition between the novel bursting patterns if the excitation amplitudes vary. In particular, such a transition exhibits a complex evolution process, which has been found to be related to the fact that the number of delay-induced hysteresis behaviors in the compound pitchfork-hysteresis bursting varies with the excitation amplitudes. However, effective theories and methods for analyzing the intrinsic mechanisms of the effects of amplitudes on delay-induced hysteresis behaviors in bursting patterns are still missing and need to be developed.

All the bursting patterns studied here are based on rationally related excitation frequencies. If the excitation frequencies are incommensurate, then a complex slow variable $g(t) = \beta_1 \cos(\omega_1 t) + \beta_2 \cos(\omega_2 t)$, whose "period" is infinitely long, is obtained. For this case, the slow variable $g(t)$ can increase through the pitchfork bifurcation point numerous times within one "period." As we have seen, an increase through the pitchfork bifurcation point may lead to a simple bursting pattern with one single delayed bifurcation. Therefore, compared to the same system with rationally related excitation frequencies, the Duffing system with incommensurate excitation frequencies may exhibit complex bursting patterns with more bifurcations. However, note that the method given in Ref. 22 requires that the excitation frequencies should be rationally related. Therefore, new technologies or methods need to be developed in order to reveal bifurcations and fast transitions in complex bursting patterns related to incommensurate excitation frequencies. This is an open problem for further research.

Finally, we would like to point out that here all the bursting structures are obtained by using the classical Runge-Kutta method.[33] With integration methods with low orders (e.g., the Euler method[33]), the bursting structures, however, may disappear, and therefore, they are sensitive to numerical methods. We would also like to point out that, because bifurcation delay can be shortened by noise,[14] bursting structures with shortened delay behaviors may be observed if noise is introduced into the system. In particular, because bifurcation delay can be observed in experiments,[34,35] the bursting structures reported here, which depend heavily on bifurcation delay, may be encountered experimentally, although no direct examples have been found yet.

ACKNOWLEDGMENTS

The authors express their gratitude to the editor and the anonymous reviewers whose comments and suggestions helped in the improvement of this paper. This work was supported by the National Natural Science Foundation of China (Grant Nos. 11572141, 11632008, 11772161, and 11502091) and the Training Project for Young Backbone Teacher of Jiangsu University.

[1]M. Desroches, J. Guckenheimer, B. Krauskopf, C. Kuehn, H. M. Osinga, and M. Wechselberger, SIAM Rev. **54**, 211 (2012).
[2]J. Y. Hou, X. H. Li, and J. F. Chen, J. Vibroeng. **18**, 4812 (2016).
[3]A. Vidal, Lect. Notes Control Inf. Sci. **341**, 439 (2006).
[4]G. V. Savino and C. M. Formigli, Biosystems **97**, 9 (2009).
[5]E. M. Izhikevich, IEEE Trans. Neural Networks **14**, 1569 (2003).
[6]S. Liepelt, J. A. Freund, L. Schimansky-Geier, A. Neiman, and D. F. Russell, J. Theor. Biol. **237**, 30 (2005).
[7]Q. S. Lu, H. G. Gu, Z. Q. Yang, X. Shi, L. X. Duan, and Y. H. Zheng, Acta Mech. Sin. **24**, 593 (2008).
[8]A. N. Pisarchika and U. Feudel, Phys. Rep. **540**, 167 (2014).
[9]M. Krupa, A. Vidal, M. Desroches, and F. Clément, SIAM J. Appl. Dyn. Syst. **11**, 1458 (2012).
[10]R. Curtu, Physica D **239**, 504 (2010).
[11]O. V. Maslennikov and V. I. Nekorkin, Chaos **23**, 023129 (2013).
[12]X. J. Han, F. B. Xia, C. Zhang, and Y. Yu, Nonlinear Dyn. **88**, 2693 (2017).
[13]C. Kuehn, *Multiple Time Scale Dynamics* (Springer, Berlin, 2015).
[14]E. M. Izhikevich, Int. J. Bifurcation Chaos **10**, 1171 (2000).
[15]H. Simo and P. Woafo, Mech. Res. Commun. **38**, 537 (2011).
[16]X. H. Li and J. Y. Hou, Int. J. Nonlinear Mech. **81**, 165 (2016).
[17]Z. Rakaric and I. Kovacic, Mech. Syst. Signal Process. **81**, 35 (2016).

[18]X. J. Han and Q. S. Bi, Commun. Nonlinear Sci. Numer. Simul. **16**, 4146 (2011).
[19]M. Golubitsky, K. Josic, and T. J. Kaper, in *Global Analysis of Dynamical Systems: Festschrift Dedicated to Floris Takens on the Occasion of his 60th Birthday*, edited by H. W. Broer, B. Krauskopf, and G. Vegter (Institute of Physics, Bristol, 2001), pp. 277–308.
[20]H. M. Osinga, A. Sherman, and K. Tsaneva-Atanasovac, Discrete Contin. Dyn. Syst. Ser. A **32**, 2853 (2012).
[21]M. L. Saggio, A. Spiegler, C. Bernard, and V. K. Jirsa, J. Math. Neurosci. **7**, 7 (2017).
[22]X. J. Han, Q. S. Bi, P. Ji, and J. Kurths, Phys. Rev. E **92**, 012911 (2015).
[23]X. J. Han, Y. Yu, C. Zhang, F. B. Xia, and Q. S. Bi, Int. J. Nonlinear Mech. **89**, 69 (2017).
[24]G. J. M. Maree, SIAM J. Appl. Math. **56**, 889 (1996).
[25]N. Berglund and H. Kunz, Phys. Rev. Lett. **78**, 1691 (1997).
[26]X. J. Han, Q. S. Bi, C. Zhang, and Y. Yu, Int. J. Bifurcation Chaos **24**, 1450098 (2014).
[27]X. J. Han and Q. S. Bi, Sci. China Technol. Sci. **55**, 702 (2012).
[28]L. X. Duan, Q. S. Lu, and Q. Y. Wang, Neurocomputing **72**, 341 (2008).
[29]Q. S. Lu, Z. Q. Yang, L. X. Duan, H. G. Gu, and W. Ren, Chaos Solitons Fractals **40**, 577 (2009).
[30]B. Ibarz, J. M. Casado, and M. A. F. Sanjuán, Phys. Rep. **501**, 1 (2011).
[31]O. V. Maslennikov and V. I. Nekorkin, Chaos **26**, 073104 (2016).
[32]X. J. Han, Y. Yu, and C. Zhang, Nonlinear Dyn. **88**, 2889 (2017).
[33]J. C. Butcher, *Numerical Methods for Ordinary Differential Equations* (Wiley, New York, 2008).
[34]E. Jakobsson and R. Guttman, "Continuous stimulation and threshold of axons: The other legacy of Kenneth Cole," in *The Biophysical Approach to Excitable Systems*, edited by W. J. Adelman and D. E. Goldman (Plenum, New York, 1981), pp. 197–211.
[35]J. Z. Su, "The phenomenon of delayed bifurcation and its analyses," in *Multiple-Time-Scale Dynamical Systems*, edited by C. K. R. T. Jones and A. I. Khibnik (Springer, New York, 2001), pp. 203–214.